Topology and Parameter Estimation in Power Systems through Inverter Based Broadband Stimulations

Surena Neshvad [1*], Harag Margossian [1], Jürgen Sachau [1]

[1] Interdisciplinary Center for Security, Reliability and Trust, University of Luxembourg, Luxembourg
surena.neshvad@uni.lu

Abstract: An increasing number of inverter based power generators have been connected to the distribution network in recent years. This phenomenon, coupled with the adoption of open energy markets has significantly complicated the powerflows on the power network, requiring advanced and intelligent parameter knowledge to optimize the efficiency, quality and reliability of the system. This paper describes a method for identifying parameters associated with the power system model. In particular, the proposed algorithm in this paper addresses the line parameter and topology identification task in the scope of state estimation. The goal is to reduce the a priori knowledge for state estimation, and to obtain online information on the power system network. The proposed parameter estimation method relies on injected stimulations in the network. Broadband stimulation signals are injected from distributed generators and their effects measured at various locations in the grid. To process and evaluate this data, a novel aggregation method based on weighed least-squares will be proposed in this paper. It combines and correlates various measurements in order to obtain an accurate snapshot of the power network parameters. In order to test its capabilities, the performance of this algorithm is evaluated on a small-scale test system.

1. Introduction

The mathematical model of the power system is utilized by Energy Management System (EMS) applications in the elaboration of their algorithms. Examples of such parameters are transmission line parameters, status of power switches and status of Distributed Generators (DG) [1]. The most important EMS tool is state estimation, but other state-of-the-art tools such as network topology reconfiguration [2], adaptive feeder protection in presence of DG [3-4] use this model as well in order to optimize powerflows and guarantee proper behaviour of the protective devices.

Traditional state estimation is performed under the assumption that all the network parameters are assessed correctly, and that state estimation inconsistencies are due to inaccurate measurements. But errors may also be due to topology or parameter errors, which can lead to correlated measurement divergence and deteriorate results [5-6]. Many factors can influence the reliability and precision of the network

parameter models. Meteorological conditions such as temperature and humidity along the line can have considerable impact [7]. Geographical properties, including vegetation and soil do have a substantial influence as well. In classical approaches, as described in [7-8], an estimation of these parameters is calculated offline in order to model their influence on the line parameters, assuming all other factors known, such as tower and cable geometric parameters. However a large amount of precise data is required for an adequate estimation of line parameters and the research in [5] has shown that a large number of in service power lines have values that poorly reflect the real measured impedance.

Several parameter estimation methods have been researched and they are mostly based on modifications of existing state estimation algorithms. The first group of research analyses the residual of the state estimation procedure and looks for correlation patterns, linking measurement residuals to parameter errors [9-12]. This analysis is performed once state estimation is complete, and is added as an extra step to the algorithm. The second group of methods uses an extended state vector and constraints on the system in order to identify the parameters to be discovered [13-14]. Additionally, research in [15] uses a Bayesian approach to identify relevant topological changes, through a second level processing of the state estimation algorithm. The method proposed in [16] adds additional soft constraints, modelled as pseudo-constraints for generalized state estimation in order to identify the correct network configuration.

The research in this paper considers a novel parameter estimation method based on active identification [17-19]. The proposed method distorts the voltage at the DG by injecting a broadband stimulation, measures the current response to those signals, and obtains relevant information through correlation between the stimulation and its response. Active identification at the inverters Point of Common Coupling for estimating the equivalent impedance seen from the inverter has been studied in the past [20-21]. In this research the harmonic rich currents generated at the inverter are additionally measured at nearby locations in the power network. The identification method utilized in this research relies on stimulations injected through a Pulse Width Modulator (PWM); it creates an excitation signal based on the research in [22] in which Pseudo Random Binary Sequences (PRBS) signals have been used to create harmonic-rich stimulations. Stimulation signals sent from various sources in the power system are measured at several locations in order to estimate the transfer function of their propagation paths. All the measurement results are then combined using a network parameter model based on the power system's admittance matrix and a Weighed Least Square (WLS) algorithm is applied in order to infer the unknown system variables.

This paper is structured as follows: In Section 2, the proposed active identification method based on PRBS patterns is described. The stimulation injection method applied on PWM based inverters is

presented, and a system parameter estimation method based on multiple concurrent measurements is proposed. In Section 3, a novel WLS-based algorithm, applied on the system's admittance matrix is elaborated, and the application of the method on a distribution network is depicted. Section 4 illustrates simulation results for practical system settings and provides an analysis on system convergence and result accuracy.

2. Proposed Method

2.1 Stimulation Signal Attributes

Pseudo-Random Binary Sequences are deterministic bit streams of '1's and '0's occurring 'pseudo-randomly' over their run length, after which the sequence is repeated. Due to their mathematical properties, they are a valuable stimulation signal for active system identification [17]. For the specific case of Maximum Length Sequences (MLS) and for a given seed, a polynomial of length L will generate a deterministic sequence of '1's and '0's of $2^L - 1$ elements [23]. Depending on the relationship between the code-length, sampling frequency and code frequency, the PRBS exhibits a 'white noise-like' spectrum for a defined frequency range, with zeros occurring at multiples of the PRBS clock sampling frequency. The code length and its sampling frequency limit the resolution of the stimulated spectrum. The logic required for PRBS implementation consists of shifters and XORs and can be easily implemented on a modest digital controller. An additional advantage of PRBS is that even very low amplitude stimulations can produce accurate estimation results, since its effect is aggregated over a complete PRBS run length.

For short time intervals, power systems can be assumed to be steady-state linear time-invariant system. The system's response to a PRBS stimulation can be represented by the following equation:

$$y(n) = \sum_{k=1}^{\infty} h(k)u(n-k) + v(n) \qquad (1)$$

Where $y(n)$ is the output signal of the system, $h(k)$ the impulse response of the system to be identified, $u(k)$ the input signal, which is the PRBS pattern in our case, and the disturbances, modeled by white noise are represented by v(k).

The cross correlation of the input signal with the output signal is given by:

$$R_{uy}(m) = \sum_{n=1}^{\infty} u(n)\, y(n+m) \qquad (2)$$

$$= \sum_{n=1}^{\infty} h(n)R_{ii}(m-n) + R_{iw}(m) \qquad (3)$$

- $R_{ii}(m)$ being the autocorrelation of the signal, and
- $R_{iw}(m)$ its correlation with uncorrelated noise

When the PRBS pattern is long enough, it exhibits white noise correlation properties [23]. Thus $R_{ii}(m)$ becomes a Kronecker delta $\delta(m)$, while $R_{iw}(m)$ becomes zero.

$$\begin{cases} R_{ii}(m) = \delta(m) \\ R_{iw}(m) = 0 \end{cases} \qquad (4)$$

Combining (3) and (4) the cross correlation is reduced to:

$$R_{uy}(m) = h(m) \qquad (5)$$

The PRBS signal can be detected in noise magnitudes stronger than itself by a correlator who knows its sequence. This also means that multiple PRBSs can coexist and can filter each other's interference through correlation. The transfer function of the studied system in frequency domain can then be derived by applying the Fourier transform to $R_{uy}(m)$.

2.2 Signal Injection Method

A typical PWM generation controller for a single phase grid-tie inverter is shown in Figure 1. The resulting PWM control signal is used to steer an H-bridge inverter. Additional information on the structure and operation of a three level Pulse Width Modulator is can be found in [28]. In order to superimpose the PRBS on the 50 Hz fundamental, the PWM carrier is altered in a way that the generated pulse pattern naturally overlaps the PRBS with the reference signal. This is achieved by attributing a PRBS code to each carrier switching cycle. As shown in Figure 1, a percentage of each cycle is attributed to the PRBS signal.
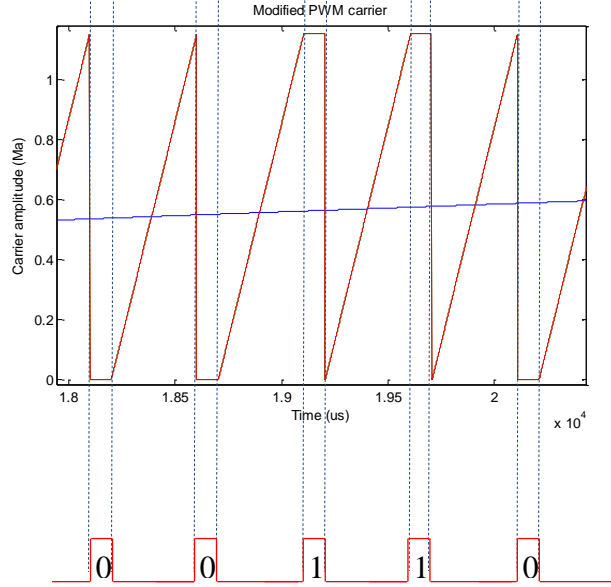
Figure 1: Implementation of a PRBS pattern on inverter's PWM: modified carrier sawtooth, implementing a '0 0 1 1 0' code

In order to generate a '0' code, the carrier is set during the PRBS duty cycle to above the maximal value of the reference signal. For a '1' PRBS code the carrier is set to 0, so that the PWM always triggers in that period. This will generate slightly 'wider than normal' pulses during for '1' codes, and slightly narrower pulses during '0' codes. The PRBS duty cycle is very small and generates low amplitude, broad spectrum harmonics. In Section 4, the PRBS burst is injected over 16 fundamental cycles, with a PRBS duty cycle of 5%. The PRBS pattern is generated without additional switching losses and without additional hardware. The code frequency is set to the PWM's switching frequency. This alteration will induce extra harmonics on the power network, similar to other proposed active identification methods proposed e.g. for islanding such as in [20]. In order to limit the harmonics injected, the PRBS injection should consist of short and low amplitude bursts, which are repeated periodically e.g. once every 5 minutes.

2.3 Mathematical model and algorithm

The objective in this section is to relate the PRBS voltage harmonics and their induced current measurement to a mathematical model of the network.

2.3.1 Transfer function estimation from measurements:

For the proposed method, PRBS patterns are injected from DGs present on the network, and the resulting current patterns are measured at various points in the grid. Previous research in [22] has shown

that the presence of PRBS can be detected through continuous correlation. Knowing beforehand the length and the codes of the sequence, the correlation peak allows us to determine precisely the time and the duration of the received pattern. The establishment of the transfer function relating the PRBS voltage patterns to the measured current patterns is done by applying equation (3) to the measured current harmonics. The equations (6-9) show the results of this operation for the described model, $h(n)$ being the transfer function of the propagation path, and R_{sr} the autocorrelation of the stimulation. The cross-correlation between the voltage stimulation and the resulting current at the receiver can be written as:

$$(v_s * i_r)(\tau) = \int_{-\infty}^{+\infty} v_s{}^*(t) i_r(t + \tau) \qquad (6)$$

For discrete measurements, the cross correlation of the PRBS duration is defined as:

$$(v_s * i_r)(n) = \sum_{n=start\_prbs\_idx}^{end\_prbs\_idx} v_s(n) i_r(n + m) \qquad (7)$$

$$= \sum_{n=start\_prbs\_idx}^{end\_prbs\_idx} h(n) R_{sr}(m - n)$$

Transposed to the frequency domain, the following equations are obtained, relating the transfer function to the input stimulation and its response:

$$\overline{V_s} \times I_r = \overline{V_s} \times (H \times V_s) = H \times |V_s|^2 \qquad (8)$$

$$H = \frac{\overline{V_s} \times I_r}{|V_s|^2} \qquad (9)$$

where $\overline{V_s}$ represents the complex conjugate of the Discrete Fourier Transform of the voltage at the source during the length of the PRBS, I_r represents the Discrete Fourier transform if the current at the receiver for the duration of the PRBS, H the discrete transfer function of the propagation path.

2.3.2 Model Based System Parameter Estimation:

The power grid is considered to be a complex grid of networked components. Due to the slow dynamics and high inertia of power systems, the system will be considered invariant during the stimulation injection. Also, due to the orthogonality property of the PRBS signal, it is also assumed that interferences between stimulations and other signals are effectively filtered out. Thus, in the elaboration of mathematical model, it will be assumed that only one PRBS stimulation signal is present as an active injection signal during its time period.

The sources inject broadband stimulation patterns on the power network. There are N injecting emitters on the network, and the matrix V_S represents the Discrete Fourier transform of all voltage stimulations. At the M receivers, the resulting broadband current is measured and is correlated with the PRBS codes of the N senders according to equations (3). A correlation peak is detected when the signal is present. The transfer function between the emitter and the receiver is established based on (6-9). As the PRBS stimulates a wide frequency band, this relation can be established for a range of frequencies up to several kHz, above which the spectral content of the PWM based PRBS wanes off and identification becomes challenging. Figure 2 illustrates the general configuration of the system and the problem to be solved.
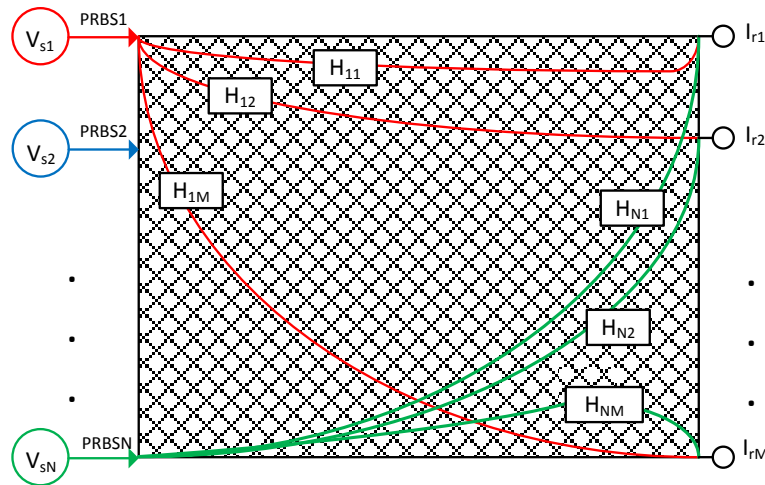

Figure 2: Power Network Identification through voltage stimulation and current measurements

For each source V_{SK} , the relationship between the source and the receivers is defined by the matrix of the injections in network :

$$\overline{V_{sk}} = \sum_{i=1}^{M} H^{-1}{}_{ik} \times I_{ki} \tag{10}$$

where

$$\overline{V_s} = \begin{bmatrix} \overline{V_{s1}} \\ \overline{V_{s2}} \\ \vdots \\ \overline{V_{sN}} \end{bmatrix} \tag{11}$$

$$H = \begin{bmatrix} H_{11} & H_{12} & \cdots & H_{1M} \\ H_{21} & H_{22} & \cdots & H_{2M} \\ \vdots & \vdots & & \vdots \\ H_{N1} & H_{N1} & \cdots & H_{NM} \end{bmatrix} \tag{12}$$

$$I_r = \begin{bmatrix} Ir_{11} & Ir_{12} & \cdots & Ir_{1N} \\ Ir_{21} & Ir_{22} & \cdots & Ir_{2N} \\ \vdots & \vdots & & \vdots \\ Ir_{M1} & Ir_{M2} & \cdots & Ir_{MN} \end{bmatrix} \tag{13}$$

Each of the N emitters creates a current stimulation at each of the M receivers. Thus an NxM matrix of transfer function is established in order to characterize the dynamic relationship between each sender and receiver. This matrix H shown in (12), characterizes the transfer functions of each path shown in Figure 2. On the other hand, the electrical dynamics of the power network are described by its admittance matrix as well. In order for the H matrix to correspond to the admittance matrix, the following changes are performed, assuming that the power network under study has K nodes, where $K > N$ and $K > M$.

- The V_S matrix is modified to a matrix of K elements, with zeros injection on nodes without PRBS stimulation.
- The current measurement at the node of each emitter corresponds to the equivalent voltage stimulation and e.g. Ir_{31} represents the current measured at node 3, resulting from stimulation from node 1. The current resulting from the PRBS at the DG is measured and evaluated.
- The I_r matrix is expanded to a KxK matrix, with 0 values on power network nodes without measurement.

For topology identification, the goal is to identify relay settings and DG connection settings. An infinite impedance models a line with an open relay setting. For a closed relay setting, the impedance of the powerline itself is considered in the admittance matrix. Thus, each element of the admittance matrix will be composed of line admittances, loads, source admittances, with binary unknowns related to each of the relay settings to be discovered. These binary values depend on the connection status of the relays and DG status. The configuration of system under study will look as depicted in Figure 3 and the equations to be solved are rewritten for a given frequency ω in equation (14).
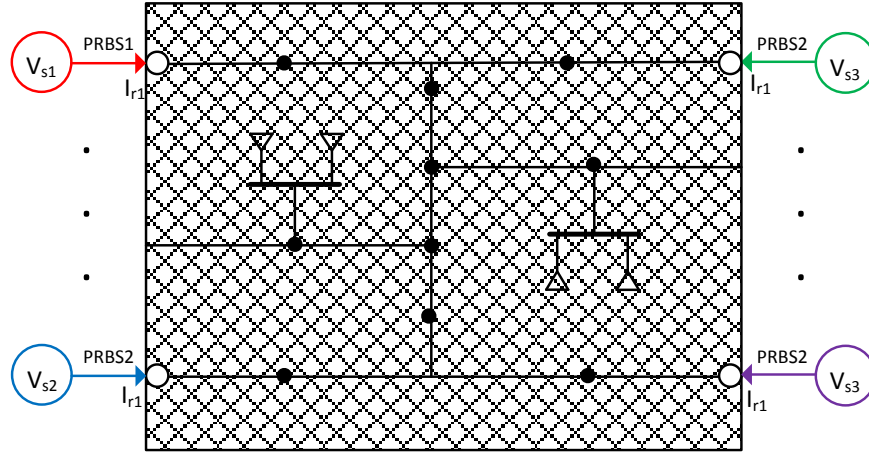

Figure 3: System identification in power network, using voltage sources as pilot injectors

The equations to be solved for each frequency ω are:

$$\overline{V_{sk}(\omega)} = \sum_{i=1}^{K} Ymatrix^{-1}{}_{ik}(\omega)_{loads,sources,lines,relays} \times Ir_{ki}(\omega) \tag{10}$$

In the next sub-section, a Weighed-Least-Squares method will be applied for the iterative estimation of the unknown parameters.

3. Weighed-Least Squares Based Solution

3.1 Overview of WLS algorithm

A measurement model to be solved can be written as:

$$z = h\left(l_p, t_p, c_p\right) + e \qquad (15)$$

where z is the measurement vector, $h\left(l_p, t_{p,} c_p\right)$ is the nonlinear function relating the measurements to the system parameters, consisting in the case under study of line parameters, topology and connection parameters, l_p is the vector containing network line parameters, t_p is the vector containing network topology and connection parameters, c_p is the vector of DG connection parameters, and e is the vector of measurement errors.

There are m measurements and n variables to be determined, with the over-specification constraint that $n < m$. The WLS parameter estimation can be formulated mathematically as an optimization problem with a quadratic objective function with additional equality constraints implemented as pseudo-measurements, the residual being defined as:

$$r = z - h(x, p) \qquad (16)$$

The goal is to minimize the objective function:

$$J(x, p) = \sum_{i=1}^{m} \frac{(z_i - h_i(x))^2}{R_{ii}} \qquad (17)$$

$$= [z - h(x, p)]^T R^{-1} [z - h(x, p)]$$

where R is the convariance matrix, related to the estimated accuracy of each measurement. The minimum of the objective function can be obtained if:

$$g(x) = \frac{dJ(x)}{dx} = -H^T(x) R^{-1} [z - h(x)] \qquad (18)$$

$$= 0$$

$H(x)$ being the Jacobian of matrix $h(x)$

$$H(x) = \left[\frac{dh}{dx}\right] \qquad (19)$$

Expanding g(x) into its non-linear Taylor series, one obtains:

$$g(x) = g(x^k) + G(x^k)(x - x^k) + \cdots \qquad (20)$$
$$= 0$$

Neglecting the higher order terms leads to an iterative solution scheme known as the Gauss-Newton method as shown below:

$$x^{k+1} = x^k - [G(x^k)]^{-1} \cdot g(x^k) \qquad (21)$$

where k is the iteration index, x^k is the solution vector at iteration k

$$G(x) = \frac{dg(x^k)}{dx} = H^T(x^k) \cdot R^{-1} \cdot H(x^k) \qquad (22)$$

$$g(x^k) = -H^T(x^k) \cdot R^{-1} \cdot (z - h(x^k)) \qquad (23)$$

The iterative process is usually stopped once convergence is assumed, that is for a threshold ϵ, once

$$|\Delta x^k| \leq \epsilon \qquad (24)$$

3.2 Application to model under study and algorithm steps

In the application of WLS to the system defined in Section 2, the measured parameters are the resulting current harmonics, which provide the transfer function for each propagation path, through the application of equations (8-9). The function relating measurements to system parameters is the modified admittance matrix which contains the following unknowns:

- Line parameters l_p
- Switch settings t_p
- DG connection status c_p

$$h(l_p, t_p, c_p) = Ymatrix(l_p, t_p, c_p) \qquad (25)$$

These parameters are being guessed initially, and the estimation is refined though the iterative process. The Jacobian of the inverse of the admittance matrix is computed for each parameter and the iterative

11

process adjusts the unknown variables in order to minimize the residual. Thus, the objective function is minimized according to the equations (20-25). The weight (inverse of covariance) for each measurement is set based on the reliability of the measurement, which is related to the magnitude of the cross correlation peak [22]. The values for the weights can therefore be dynamically computed for each measurement. Given the broadband nature of the PRBS, the parameter estimation can be operated for a wide range of frequencies. Thus the WLS algorithm can be repeated for several harmonics, in order to provide additional data points for confirming the switch settings, and in order to provide additional information on the broad spectrum dynamics of the power network components.

In the system under study, there are four PRBS injectors, acting as senders, and five receivers, detecting and measuring each of the current harmonics produced by these senders. There are a total of 11 unknowns to be determined (5 connections settings, 6 line impedance values) and 20 equations linking those unknowns for each frequency. In addition, given the broadband nature of the injected stimulation, these operations can be performed over multiple frequencies.
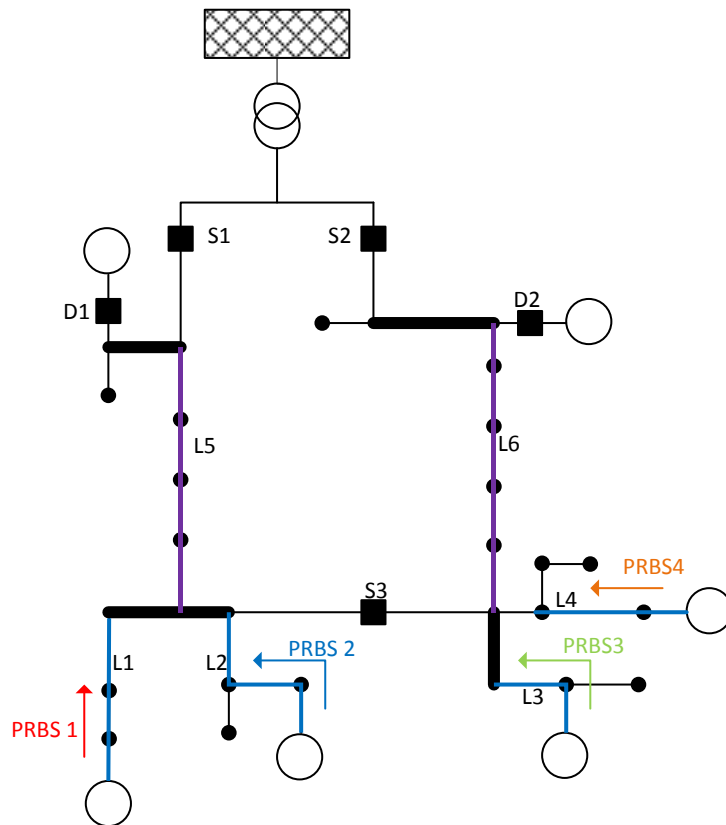

Figure 5: Example of a distribution network to be characterized

While traditional WLS can be applied to this system, instabilities might arise due to the binary nature of the switch setting parameters. In addition, the highly non-linear system may lead to inaccurate values due to local minima reached by the WLS algorithm, in conjunction with measurement noise caused by imperfect cancellation of existing interference and harmonics. The WLS algorithm is executed over a range of frequencies and the redundancy of these multiple WLS runs is exploited in order to perform the identification sequentially and obtain the parameters serially. In order to optimize the results, the following sequence is executed by splitting the topology and parameter detection is distinct steps:

- In the first instance, line parameters are assumed to be known within 30% of their actual value. The WLS equations are solved with the only unknown parameters being the switch settings and DG connection parameters. The algorithm is executed over the frequency range of 80 – 1980 Hz in 100Hz intervals, and the average of the converged estimates, rounded up/down and weighed with the final residual, are assumed to accurate.

- In a second step, the line impedances are determined. The WLS algorithm is run on the 80 – 1980 Hz range, with fixed relay settings in order to estimate the impedance magnitude for each stimulated line on the studied frequency range.

- Finally, the complete WLS algorithm is re-executed, with the previously obtained values used as an initial guess for the unknown parameters, and a rapid convergence should be obtained if the previous estimates are accurate.

In the next section, the described model and the defined algorithm are executed on Simulink and Matlab, in order to illustrate the feasibility and performance of the proposed method.

4. Simulation Results

Simulations are based on the system described in Section 2 and Section 3. The model is executed on Simulink/Matlab for PRBS injection, correlation estimation and WLS algorithm. The characteristics of the system to be estimated, including stimulation parameters and receiver settings are listed in Table 1. The network considered for the application of the algorithm is the one depicted in Figure 5. The output filters of all DGs are LC filters and their admittances *Yf* are assumed to be identical. The unknown parameters in the system are the switch settings *S1- S3*, DG connection status connection status *D1-D2* and the line impedances *Y1-Y6*, consisting of a resistive and inductive component.

In the studied system, the feeders are branched twice to distribute power to the loads. Under normal operation, the complete network can be fed through feeder 1, feeder 2 or both depending on the status of

the switches *S1*, *S2* and *S3*. Additionally a meshed network can be produced if all switches are connected. *DG1*, *DG2*, *DG3*, and *DG4* are monitoring DGs. They inject periodically PRBS sequences on the network. The connection status of *D1* and *D2* is intermittent and not known by the operator. The objective of the topology identification algorithm is to evaluate the status of the switches *S1*, *S2* and *S3* as well as the connection status *D1* and *D2*. In a second step, the measurement data is processed in order to estimate the parameters of all the lines in the network.

Connected to each node on each feeder are residential loads. For typical residential loads, the relative high equivalent impedance has a minimal impact on harmonic current flows and ignoring it doesn't modify the estimations considerably. On the other hand, loss of large loads or DG disconnects can be considered a critical change. The equivalent impedance of the MV transformer and upstream grid is chosen according to [24], a resistive-inductive model is used for the substation transformer, since capacitive effects and leakage inductance a relative small compared to the magnetizing inductance in the studied frequency range [25].

DG1-DG4 will be injecting PRBS patterns on the power network. The injections are orthogonal, thus their interference will be minimal if concurrent injection from two DGs happens. Using equations (8-9), the transfer function between the emitter and the receiver can be established. The PRBS stimulates a wide frequency band and this relation can be established for all the stimulated frequencies. The intended frequency identification range is up to 2000 Hz, since typically the first forty harmonics are considered for power quality considerations in European grid codes [26].

Table 1: System Parameters

Stimulation parameters	
PRBS code length	4093
PRBS polynomial node 1	$x^{12} + x^8 + x^2 + x + 1$
PRBS polynomial node 2	$x^{12} + x^6 + x^4 + x + 1$
PRBS polynomial node 3	$x^{12} + x^6 + x^5 + x^3 + 1$
PRBS polynomial node 4	$x^{12} + x^7 + x^6 + x^2 + 1$
Sampling frequency	50 KHz
Carrier frequency	12800 Hz
Codes per fundamental cycle	256
PRBS amplitude p.u.	5 %

Electrical system params

Line 1 impedance Zl1	0.1 Ω , 2 mH
Line 2 impedance Zl2	0.3 Ω , 6 mH
Line 3 impedance Zl3	0.2 Ω , 1 mH
Line 4 impedance Zl4	0.1 Ω , 2 mH
Line 5 impedance Zl5	0.3 Ω , 3 mH
Line 6 impedance Zl6	0.1 Ω , 1 mH
Line 7 impedance Zl7	0.2 Ω , 2 mH
Inverter Output filter Zc – Zf	5 Ω , 9.45e1μF - 10 mH
Transformer Impedance Zt	0.12 Ω , 20 mH
Switch settings	SW1 = 1, SW2 = 0, SW 3= 1
DG connection setting	DG1=0, DG2 = 1

The polynomials of the PRBS codes emitted from each DG are shown in Table 1. They represent orthogonal 12-bit PRBS sequences and each generates a sequence of 4093 symbols before it repeats itself. In the simulation settings, the signals are concurrent, thus, interference between signals is maximal. The current measurements are sampled at the receivers at 50 kHz, which is 25 times above the highest studied frequency. The inverter's carriers producing the stimulation have a switching frequency of 12800 Hz. Therefore each period of the fundamental takes 256 pulses, and 256 PRBS codes are transmitted during each fundamental. A PRBS cycle takes 16 50 HZ cycles to complete. The duty cycle for the PRBS is set to 5% in the simulation settings. Line parameters and loads are based on the Creos power network in Luxembourg.

The first step of the algorithm is the estimation of the transfer functions correlating the PRBS injections, and measurements at various locations in the grid. The measurements are done in a noisy environment, with multiple generators running. Figure 4 shows the results of transfer function identification for PRBS from source *DG1*, *DG2*, *DG3*, and *DG4*. The straight line corresponds to the theoretical value to be obtained, based on the calculated value of the equivalent model. The noisy/colored lines are the results obtained through PRBS injection and correlation. As stated in Section 3, the weights associated to these noisier measurements will be lower in the WLS algorithm. The measurements close to the PRBS source will have higher impact during WLS, while measurements electrically far from the source provide low reliability data, associated with a small weight during WLS.
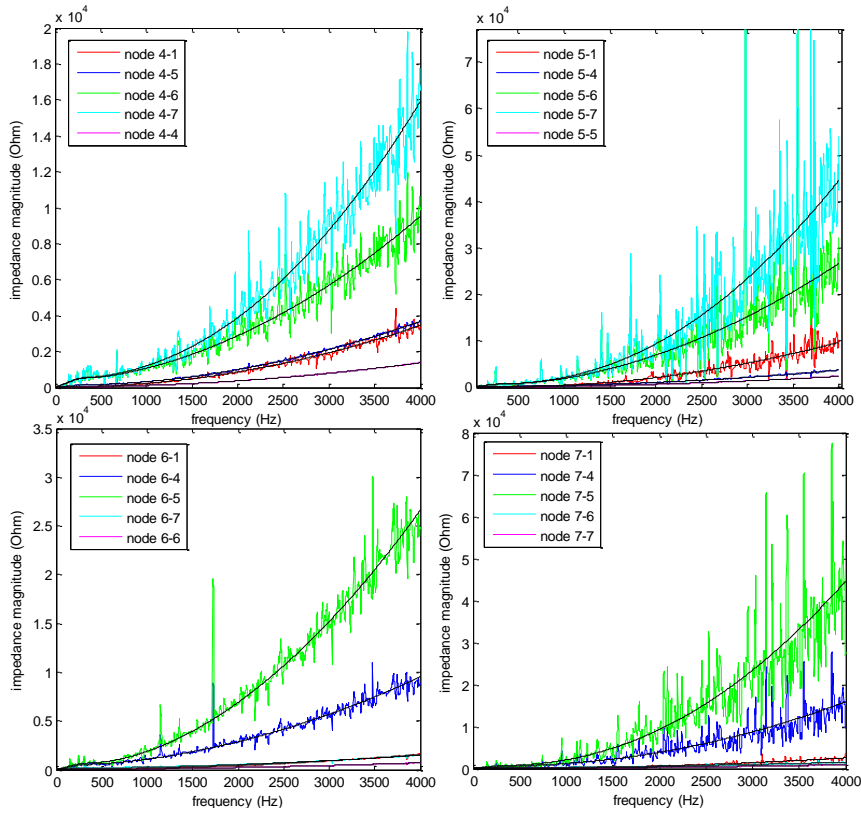
Figure 4: Theoretical and estimated transfer function from source to destination nodes

Equivalent data is collected and processed for all four PRBS sources, then evaluated. The second step of the algorithm is the estimation of the power network parameters. The data from the Simulink run, shown in Figure 4, is processed with the parameter identification algorithm, using the *Ymatrix* and the equations described in Section 2 and 3. The results of each of the two WLS runs is listed and analyzed below.

4.1 DG connection and switch status identification

The switch settings are set to '101', and the DG settings to '01': the complete network is powered by the left feeder, and the DG on node DG2 is disconnected. For the initial setting of the WLS algorithm, all parameters are set to '0.5'. The algorithm is executed on the 80-1980 Hz frequency range, with 100 Hz intervals. The results obtained by this procedure are shown in Table 1.

Table 2: Topology estimation through WLS for 80-1980Hz

S1	S2	S3	D1	D2
Real Topology values to be found				
1	0	1	0	1

	Initial WLS parameter setting						
	0.5	**0.5**	**0.5**	**0.5**	**0.5**		
Frequency	**WLS result**					**residue**	**err %**
80	0.99	0.02	0.98	0.05	0.85	0.16	8%
180	*0.95*	*0.04*	*0.57*	*0.94*	*0.02*	*1.58*	*81%*
280	0.99	0.05	1.00	0.05	0.93	0.30	6%
380	0.78	0.03	1.00	0.05	0.96	0.24	13%
480	0.85	0.01	1.00	0.95	0.05	2.65	70%
580	0.98	0.00	0.99	0.01	0.95	0.22	7%
680	0.77	0.04	1.00	0.01	0.98	0.34	16%
780	*0.77*	*0.12*	*0.97*	*0.61*	*0.05*	*0.72*	*65%*
880	0.98	0.01	0.95	0.00	0.60	0.27	17%
980	0.86	0.05	0.72	0.00	0.93	0.40	19%
1080	*0.86*	*0.03*	*0.94*	*0.82*	*0.06*	*1.10*	*66%*
1180	0.88	0.04	0.95	0.00	0.99	0.36	22%
1280	0.75	0.04	0.85	0.17	0.92	0.43	23%
1380	0.99	0.05	0.95	0.05	0.95	0.07	8%
1480	0.89	0.06	0.99	0.05	0.94	2.29	7%
1580	0.81	0.03	0.87	0.11	0.99	0.94	17%
1680	0.68	0.02	0.95	0.28	0.99	0.92	24%
1780	*0.86*	*0.10*	*0.58*	*0.95*	*0.05*	*5.94*	*85%*
1880	0.79	0.04	0.82	0.27	0.66	0.64	34%
1980	0.64	0.11	0.91	0.05	0.99	0.58	22%
Weighted average	**0.90**	**0.02**	**0.94**	**0.11**	**0.86**		**9%**

The weighted average of the result corresponds to the estimation of each parameter, associated with a weight inversely proportional to the residue at the end of the WLS run. In fact, erroneous runs typically are terminated with a high residue, and thus their contribution can be reduced without additional steps of data examination and processing. If the residues of the WLS result are above a certain threshold, the convergence is assumed to have failed and the results discarded. This has been observed for 4 frequencies out of the 20 runs, marked in italics on Table 2. The results of the final weighted average show that the

switch settings are estimated correctly, assuming that the final result will be rounded up/down. Simulations for various other settings have shown good results as well, and no additional result post processing or heuristics have been required in order to improve the WLS performance. It can be seen that for certain frequencies e.g. 1080 Hz, the WLS algorithm has converged to wrong values. This can be attributed to the highly non-linear nature of the system, since a parameter jump in the iterative procedure can lead the estimated value to an erroneous convergence. Nevertheless due the redundancy of the algorithm, this error can be tolerated, since the majority of the frequencies converge correctly and since the bad results typically end the WLS run with higher residues, making their contribution to the weighted average is less prevalent. The iteration limit was set to 15 and the tolerance to 1% of the value to be estimated. Typically, the WLS ran for the full 15 cycles, and increasing the iterations didn't improve the results considerably, mostly due to imperfect line parameter settings.

4.2 Impedance magnitude estimation

With the finalized switch and DG connection settings, the WLS procedure is run with line impedances set to unknown parameters. The outcome of the WLS algorithm for both cases is shown in Figure 5. The continuous lines represent the theoretical value to be obtained, and the dots represent the results for the WLS algorithm for each frequency. The weighed fitting line through the data, marked by the '*' dots in Figure 5 shows that the results aggregated over the complete frequency range exhibits results very close to theoretical values. The inaccuracies are minimal for most frequencies and mostly due to noise and interference, while for some frequencies (e.g. 580 Hz) the convergence fails, and the result needs to be discarded. The criteria for acceptable runs are identical as for topology identification, runs with high residues are discarded, and the very low residue runs are given higher importance. In the settings of our simulation the peak of the stimulation is 5% of the fundamental at the DG. Simulations done with as low as 3% have provided acceptable results as well.
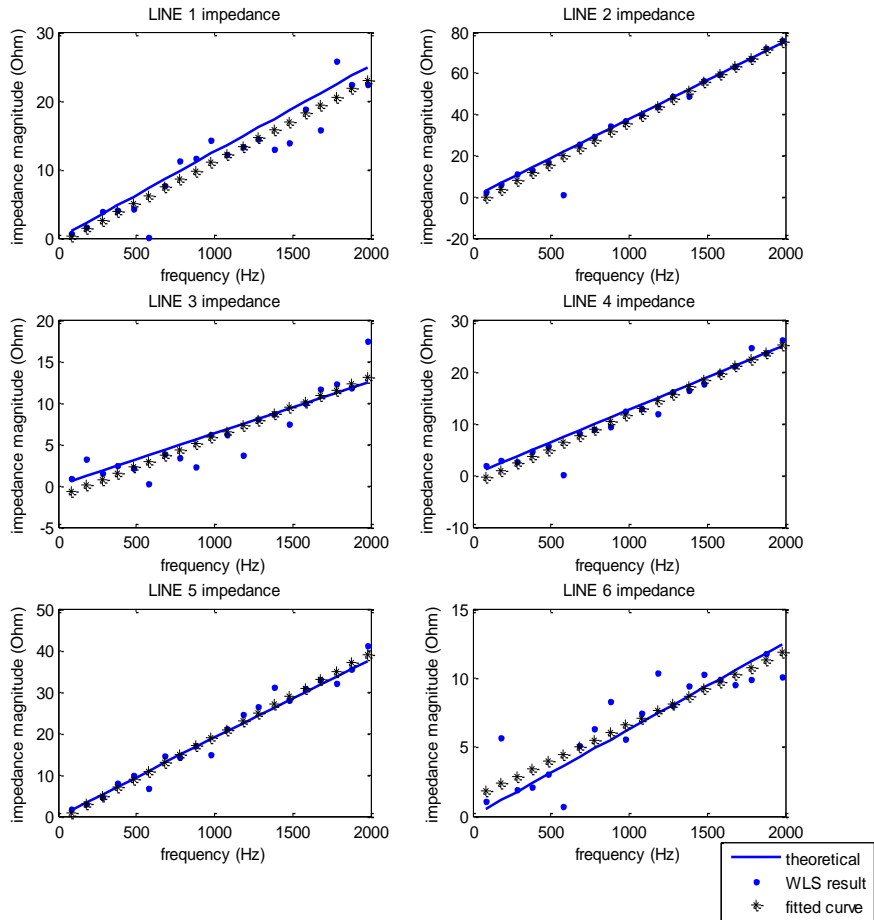
Figure 5: Line Impedance magnitudes obtained through parameter estimation

5. Conclusions

The complexity of the power network is increasing due to the large number of distributed inverter based generators. In the long term, this might have an impact on grid infrastructure stability and reliability. In this paper, a novel method has been proposed to estimate topology and line parameters of the power network using online stimulations. The method consists in injecting predefined coded stimulations from selected inverters on the grid, and measure the current response of these injections at several locations on the power network. The combination of these measurements can be exploited to compute the topology parameters and line parameters using WLS based algorithms. The proposed method can be applied to any parameters of the power system, as long as its effect on the stimulations current response can be materialized in equations.

A monitoring tool such as the one proposed in this paper can assist grid operators in supporting and accommodating modern and complex smart grid tools that are developed. For instance, the outcome of the

research can help engineers to tune the parameters of the state estimator, and optimize line usage and improve reliability by providing a novel and complementary solution to traditional EMS tools.

6. Acknowledgments

7. References

[1]   Alsac O., Vempati N., Stott B., Monticelli A.: 'Generalized state estimation [power systems]', Power Industry Computer Applications., 1997. 20th International Conference on, vol., no., pp.90, 96, 11-16 May 1997.

[2]   Bilibin I., Capitanescu F., Sachau J.: 'Overloads management in active radial distribution systems: An optimization approach including network switching', PowerTech (POWERTECH), 2013 IEEE Grenoble, vol., no., pp.1, 5, 16-20 June 2013.

[3]   Margossian H., Capitanescu F., Sachau J.: 'Distributed generator status estimation for adaptive feeder protection in active distribution grids', Electricity Distribution (CIRED 2013), 22nd International Conference and Exhibition on, vol., no., pp.1, 4, 10-13 June 2013.

[4]   Margossian H., Deconninck G., Sachau J.: 'Distribution network protection considering grid code requirements for distributed generation', Generation, Transmission & Distribution, IET, DOI: 10.1049/iet-gtd.2014.0987, April 2015.

[5]   Bockarjova M., Andersson G.: 'Transmission Line Conductor Temperature Impact on State Estimation Accuracy', Power Tech, 2007 IEEE Lausanne, vol., no., pp.701, 706, 1-5 July 2007.

[6]   U. Klapper, D. Welton, A. Apostolov, 'Why we should measure impedance', Omnicron Electronics Technical Paper, Austria, Tech. Rep. 0504, Aug. 2009, http://www.pacworld.org/, accessed 15 October 2014.

[7]   Chan S.M.: 'Computing Overhead line parameters', Computer Appl. Power, vol 6, num 1, 1993

[8]   Dommel H.W., 'Overhead Line Parameters From Handbook Formulas And Computer Programs', Power Apparatus and Systems, IEEE Transactions on , vol.PAS-104, no.2, pp.366,372, Feb. 1985.

[9]   Liu W.-H.E., Wu F.F., Shau-Ming L.: 'Estimation of parameter errors from measurement residuals in state estimation [power systems]', Power Systems, IEEE Transactions on, vol.7, no.1, pp.81, 89, Feb 1992.

[10]   Van Cutsem T., Quintana V.H.: 'Network parameter estimation using online data with application to transformer tap position estimation', Generation, Transmission and Distribution, IEE Proceedings C, vol.135, no.1, pp.31, 40, Jan 1988.

[11]   Handschin E., Kliokys, E.: 'Transformer tap position estimation and bad data detection using dynamic signal modelling', Power Systems, IEEE Transactions on , vol.10, no.2, pp.810,817, May 1995.

[12]   Souza, J.C.S., Leite da Silva A.M., Alves da Silva A.P.: 'Data visualization and identification of anomalies in power system state estimation using artificial neural networks', Generation, Transmission and Distribution, IEE Proceedings- , vol.144, no.5, pp.445,455, Sep 1997.

[13]   London J.B.A., Alberto L.F.C., Bretas N.G.: 'Analysis of measurement-set qualitative characteristics for state-estimation purposes', Generation, Transmission & Distribution, IET, vol.1, no.1, pp.39,45, January 2007.

[14]   Slutsker I., Mokhtari S.: 'Comprehensive estimation in power systems: State, topology and parameter estimation', in Proceedings of American Power Conerence., Chicago, IL, Apr. 1995, Paper 170.

[15]   Singh R., Manitsas E., Pal B.C., Strbac G., 'A recursive Bayesian approach for identification of network configuration changes in distribution system state estimation', Power and Energy Society General Meeting, 2011 IEEE , vol., no., pp.1,1, 24-29 July 2011

[16]   Korres G.N., Manousakis N.M.: 'A state estimation algorithm for monitoring topology changes in distribution systems', Power and Energy Society General Meeting, 2012 IEEE , vol., no., pp.1,8, 22-26 July 2012

[17]   Ljung L., Glad T.: 'Modeling of Dynamic Systems', Prentice Hall 1994

[18]   Papadopoulos P.N., Papadopoulos T.A., Crolla P., Roscoe A.J., Papagiannis G.K., Burt G.M.: 'Measurement-based analysis of the dynamic performance of microgrids using system identification techniques', Generation, Transmission & Distribution, IET , vol.9, no.1, pp.90,103, 1 8 2015.

[19]   Garcia-Lagos F., Joya G., Marin F.J., Sandoval F.: 'Modular power system topology assessment using Gaussian potential functions', Generation, Transmission and Distribution, IEE Proceedings- , vol.150, no.5, pp.635,640, 15 Sept. 2000.

[20]   Asiminoaei L., Teodorescu R., Blaabjerg F., Borup U.: 'Implementation and Test of an Online Embedded Grid Impedance Estimation Technique for PV Inverters', Industrial Electronics, IEEE Transactions on , vol.52, no.4, pp.1136,1144, Aug. 2005.

[21]   Langkowski H., Trung Do Thanh, Dettmann K.-D., Schulz D.: 'Grid impedance determination — relevancy for grid integration of renewable energy systems', Industrial Electronics, 2009. IECON '09. 35th Annual Conference of IEEE, vol., no., pp.516, 521, 3-5 Nov. 2009.

[22]   Neshvad S., Chatzinotas S., Sachau J.: 'Wideband Identification of Power Network Parameters Using Pseudo-Random Binary Sequences on Power Inverters', Smart Grid, IEEE Transactions on , vol.PP, no.99, pp.1,1.

[23]   Mutagi R.N.: 'Pseudo noise sequences for engineers', Electronics & Communication Engineering Journal, vol.8, no.2, pp.79,87, Apr 1996.

[24]   ABB: 'MV/LV transformer substations: theory and examples of short-circuit calculation', Technical Application Papers, February 2008, accessed 15 October 2014.

[25]   Bagheri M., Naderi M. S., Blackburn T., and Phung T.: 'Frequency response analysis and short-circuit impedance measurement in detection of winding', in Proc. Int. Conf. High Voltage Eng. Appl., Chongqing, China, 2008, pp. 33–40.

[26]   Merkmale der Spannung in Öffentlichen Elektrizitätsversorgungsnetzen, European Standard 50160, Aug. 2007, accessed 15 October 2014.

[27]   Zhou K., Wang D., 'Relationship between space-vector modulation and three-phase carrier-based PWM: A comprehensive analysis', IEEE Trans. Ind. Electron., vol. 49, no. 1, pp. 186–196, Feb. 2002.